2011

Gold nanoparticle generation using in situ reduction on a photoresist polymer substrate

Christopher J. Clukay
University of Central Florida

GOLD NANOPARTICLE GENERATION USING *IN SITU* REDUCTION ON A PHOTORESIST POLYMER SUBSTRATE

by

CHRISTOPHER J. CLUKAY

A thesis submitted in partial fulfillment of the requirements
for the Honors in the Major Program in Chemistry
in the College of Sciences
and in the Burnett Honors College
at the University of Central Florida
Orlando, Florida

Fall Term 2012

Thesis Chair: Dr. Stephen M. Kuebler

The scientific contents of this thesis will be submitted for publication as a full paper in a peer-reviewed scientific journal, which will retain the copyright.

Abstract

This report presents evidence that *in-situ* reduction of metal ions bound to a cross-linked polymer surface does not always result in nanoparticle formation solely at the interface, as is commonly assumed, but also as much as 40 nm deep within the polymer matrix. Tetrachloroaurate ions were bound using a variety of multi-functional amines to cured films of SU-8 -- a cross-linkable epoxide frequently used for micro- and nanofabrication -- and then treated using one of several reducing agents. The resulting gold-nanoparticle decorated films were examined by X-ray photoelectron spectroscopy and by plan-view and cross-sectional transmission electron microscopy. Reduction using sodium borohydride or sodium citrate generates bands of interspersed particles as much as 40 nm deep within the polymer, suggesting both the Au(III) complex and the reducing agent are capable of penetrating the surface and affecting reduction and formation of nanoparticles within the polymer matrix. It is shown that nanoparticle formation can be confined nearer to the polymer interface by using hydroquinone, a sterically bulkier and less flexible reducing agent, or by reacting the surface in aqueous media with high molecular-weight multifunctional amines, that presumably confine Au(III) nearer to the true interface. These finding have important implications for technologies that apply surface bound nanoparticles, including electroless metallization, catalysis, nano-structure synthesis, and surface enhanced spectroscopy.

Acknowledgements

This work was supported by NSF CAREER grant #0748712 and NSF-CHE grant #0809821. Additionally was also supported by the University of Central Florida's Beckman Scholars Program. I acknowledge Dr. Kuebler, Dr. Heinrich, and Dr. Elsheimer for serving on my committee and providing invaluable feedback. Additionally I would like to acknowledge Professor Florencio E. Hernandez for useful discussions concerning potential applications of this work. Please note this work has been submitted in full to a peer-reviewed scientific journal.

Dedication

I want to dedicate this to all the people who stood by me and kept me from going mad during this whole process including my parents, friends, and groupmates. Without you this thesis would never have been written. I also want to dedicate this to my thesis Chair Dr. Kuebler, without whose help and guidance I never would have been able to write this.

Table of Contents

List of Figures

Introduction

Gold nanoparticles (Au NPs) and clusters or arrays of Au NPs have a wide variety of applications, including nanofabrication, optical devices, and catalysis.[1-9] Au NPs and NP aggregates have proven particularly effective for enhancing signal via surface plasmon resonance in various spectroscopic and sensing methods.[10,11] Some applications require very small, monodisperse particles. For example, medical therapies employing metal NPs would require particle diameters below ten nanometers if they are intended to travel through the nuclear pores of eukaryotic cells.[12] Metal NPs are used as nucleation sites in electroless metallization, which is a promising approach for creating metallized micro-electromechanical (MEMS) and optical MEMS devices.[7,13-17] Several reports have discussed the formation and stabilization of monodisperse Au NPs with dimensions that could be suitable for such applications,[18-22] but many avenues remain unexplored. It is also noteworthy that these applications often involve Au NP functionalization of a polymeric surface or structure. As such, NP synthesis and surface functionalization remains an important area of research impacting many established and emerging technologies.

The conventional approach for functionalizing surfaces with NPs involves first synthesizing colloidal particles in solution, for example by the Turkevich method[7,8,10,17-19,23] or sodium borohydride ($NaBH_4$) reduction,[11,19,20,24-26] and subsequently binding them to the surface of interest. *In-situ* reduction of gold ions adsorbed onto a surface is an alternative means for generating Au NP-functionalized surfaces and devices that offers several advantages over the conventional approach.[1,2,27-31] Chief among these are the possibility for generating smaller particles, stabilization of the NPs through surface attachment, and decreased aggregation due to

immobilization on the surface.[1,31,32] Additionally, surface-bound NPs can be readily isolated from the synthesis medium or further derivitized by simple physical transfer of the supporting substrate. Despite these advantages, *in-situ* synthesis of Au NPs remains relatively unexplored, particularly as it applies to polymeric surfaces.[1-3,29,31-34]

If NP generation by *in-situ* reduction is to be applied to polymers with good control, the effects of swelling, reagent intrusion, and the uniquely microporous nature of a polymer matrix must be taken into account. To that end, this work reports how various reducing agents and surface binding agents affect the *in-situ* formation of Au NPs at the surface of cross-linked SU-8, a photoresist which is increasingly employed for micro- and nano-scale fabrication.[26,35-37] The key findings are (1) nanoparticle generation does not occur solely at the liquid-polymer interface for all reducing agents; (2) by varying the reducing agent one can favor nanoparticle generation near the surface; and (3) variation of the binding agent can limit the formation of the majority of nanoparticles to the liquid-polymer interface.

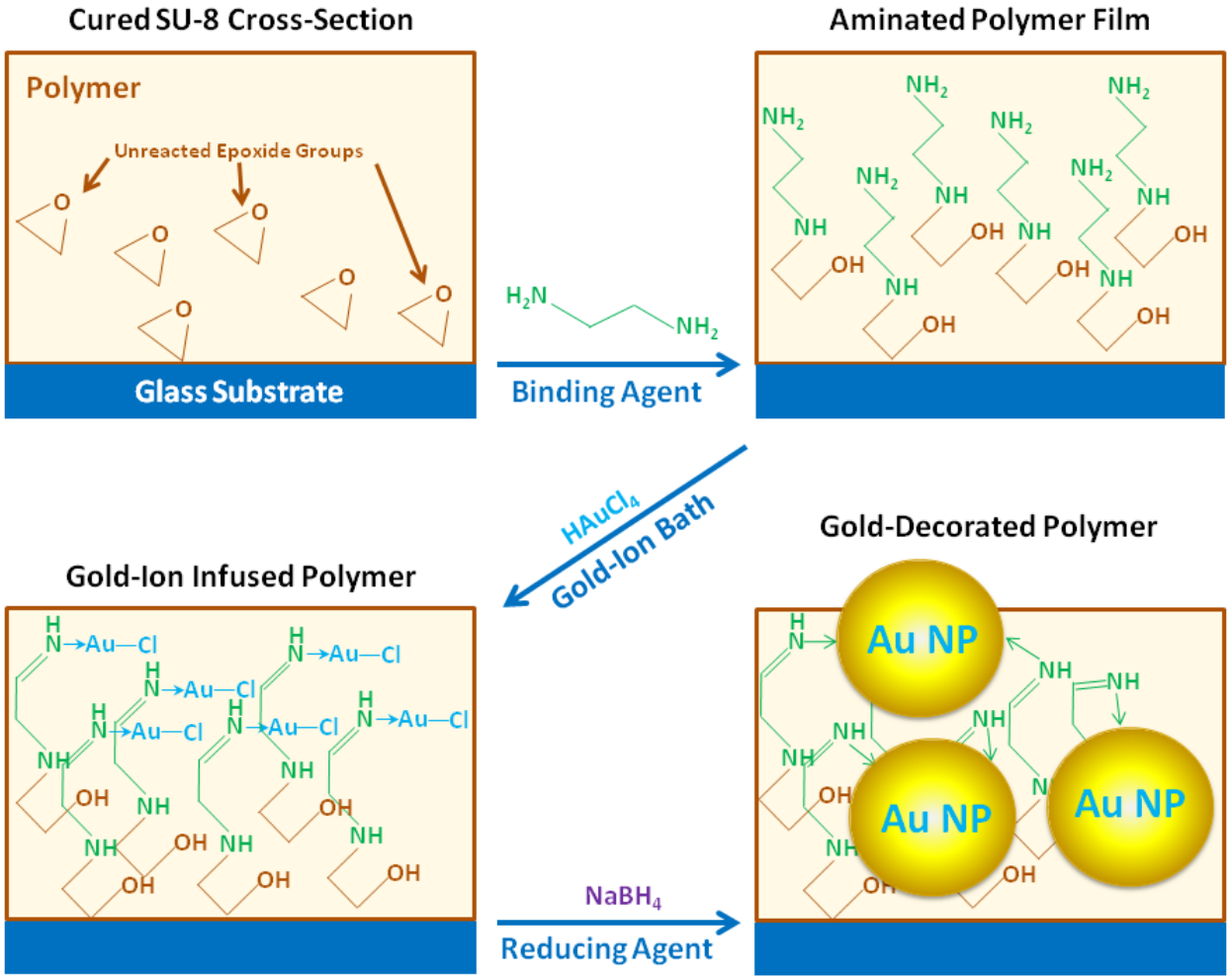

Figure 1. Process used to functionalize the surface of cross-linked polymer SU-8 with Au NPs. Each panel represents a cross-section of the film through the surface. The scheme is illustrated for the case in which Au ions are bound to the polymer film surface using ED then reduced by $NaBH_4$, and it shows but one possible mode of Au-amine interaction.

Experimental

All commercial materials were reagent grade and used as received unless otherwise indicated. Deionized water (18 MΩ) was used to rinse all sample and prepare all aqueous solutions. The process of polymer surface modification is illustrated in Fig. 1, for the case of the binding agent ethylenediamine (ED) and reducing agent $NaBH_4$. All reactions and solution preparation were carried out under ambient conditions unless otherwise stated.

2.1. Cross-linked film preparation

Square glass coverslips (25 mm, no. 1 thickness) served as substrates and were cleaned by immersion in an aqueous 1 M KOH bath (Aldrich and Fisher, technical grade) for one hour followed by drying in an oven at 100ºC for 20 minutes. Cross-linked SU-8 films were prepared by spin coating the epoxide resin (SU-8 2035, Microchem) onto cleaned substrates. Solvent was removed from the resin film by baking the samples on a hotplate. The samples were placed on a hotplate at room temperature, heated over a period of one minute to 95ºC, held at this temperature for nine minutes, then the hot plate was switched off and the samples were allowed to cool to room temperature (*circa* 10 min). The resin films were subsequently irradiated for two minutes through a long-pass filter (Omega Optical, PL-360LP, 360-nm cut off) with a broad-band UV lamp (Loctite ZETA 7411-5, 400 W metal halide source, 315 - 400 nm) then baked to activate cross-linking using the same conditions as the pre-exposure bake.

2.2. Functionalization of polymer surface with amine binding groups

Cross-linked polymer surfaces were activated toward binding Au cations by covalent attachment of a multifunctional primary amine (Fig. 2). Functionalization with ethylenediamine

(ED) was achieved by immersing the cross-linked polymer film into a 20% (v/v) of ED (Alfa Aesar, CAS# 107-15-3) in ethanol for one hour.[38,39] Functionalization with tetraethylenepentamine (TEPA, CAS# 112-57-2) and *N*-aminoethylpiperazine (AEP, CAS# 140-31-8) were similarly achieved by immersing samples in 20% (v/v) aqueous solutions of the amines for one hour. Following amination, all samples were rinsed with copious water and allowed to dry by standing in air.

2.3. Functionalization of polymer surface with gold nanoparticles

Au NP functionalized polymer surfaces were prepared by binding Au cations to aminated SU-8 films and then immediately treating with a reducing agent. The conditions selected for the reduction step were chosen to be as similar as possible to those most commonly employed for synthesis of Au NPs in solution. Amine-functionalized polymer films were placed in aqueous 5.3×10^{-4} M $HAuCl_4$ (Acros, CAS# 16961-25-4) for 30 minutes at room temperature, rinsed with copious water, then immersing into a reduction bath for 60 s consisting of aqueous 0.1 M $NaBH_4$ (Fisher, CAS# 16940-66-2).[7,19,20] Reduction using citrate was accomplished similar to the method of Khalid *et al.*[1] by immersing samples for eight hours in aqueous 1% (w/v) sodium citrate ($Na_3C_6H_5O_7$, Fisher, CAS# 6132-04-3). Reduction with hydroquinone was achieved by immersing samples for one hour in aqueous 0.1 M hydroquinone (Acros, $C_6H_4(OH)_2$, CAS# 123-31-9).[40] After reduction, samples were rinsed with copious water and allowed to dry by standing in air.

2.4. Sample preparation for transmission electron microscopy

Samples for plan-view imaging were prepared by scraping a thin section from the surface of the polymer film (*circa* 100-nm thick) and transferring it to a copper grid for imaging. For cross-sectional imaging, samples were first coated with carbon for 30 s in a vacuum evaporator (Jeol JEE 4X), to increase the contrast of the transmission electron microscopy (TEM) image and enable easy identification of Au NPs on or near the polymer surface. Each sample was then coated with Au-Pd using a sputter coater (Emitech K550) equipped with a 60-mm diameter and 0.1-mm thick magnetron target assembly. This instrument deposits metal as fine grains, without the need to cool the specimen. Sample cross-sections were prepared using a TEM focused ion beam (FIB) instrument (FEI 200) equipped with a 30 kV gallium liquid metal ion source. A 1-µm thick layer of Pt was deposited onto a rectangular strip 20 µm × 1 µm to mask the region intended for the cross-section. Through Ga-ion milling, a sample cross-section having 20-µm width, 0.15-µm thickness, and 4-µm height was obtained. A micromanipulator was then used to lift out the milled cross-section and transfer it onto a carbon-coated copper grid for TEM imaging.

2.5. Sample imaging and analysis

A Tecnai F30 operating at 300 kV was used to image samples in both plan view and cross section. Micrographs obtained from the instrument had a point-to-point image resolution of 0.2 nm. Both low magnification and high-resolution images were acquired. Energy dispersive spectroscopy (EDS) and energy filtered TEM were used to confirm that particles imaged were in fact gold. High-angle annular dark-field (HAADF) imaging in the Scanning Transmission Electron Microscopy (STEM) mode was used to analyze particle sizes. Sample

cross sections were tilted during imaging to obtain accurate minimum widths for bands of Au NP observed at or near the polymer surface.

Particle heights were obtained from calibrated HAADF-STEM pixel intensities. The projected particle area was obtained from perimeter fitting. Particle volumes were obtained from integrating HAADF-STEM pixel-intensity across the particle area. A total of 150 particles were analyzed to obtain the distribution of particle radii, heights, and volumes, and their corresponding means for a given sample. For comparison, the mean particle volume-from-height was calculated using the equation for the volume of an ellipsoid, the mean particle height, and the mean lateral radii. A given size dispersion was treated as a normal distribution and the width of the distribution is reported as a relative standard deviation (RSD) of the parameter.

2.6. X-ray photoelectron spectroscopy

Elemental composition of Au NP decorated surfaces was determined from X-ray photoelectron spectroscopy (XPS, Physical Electronics 5400 ESCA) using an unmonochromated Mg source at 15 kV potential and constant power of 300 W. Carbon was used as an internal reference[41] to correct for absolute peak shifts due to surface charging following previously reported peak locations reported for SU-8.[42] The spectra were smoothed twice using five-point averaging, corrected for linear baseline shift, and fit using a series of Gaussian-Lorentz curves (Augerscan Ver. 3.22, RBD Instruments). For peaks due to Au, each oxidation state was represented by a pair of curves separated by 3.67 eV and having curve areas locked to the 3:4 ratio expected due *f*-orbital spin-orbit coupling.[43] All curve fits were performed using least squares minimization, giving an error-mean-squared (EMS) value below 1.5.

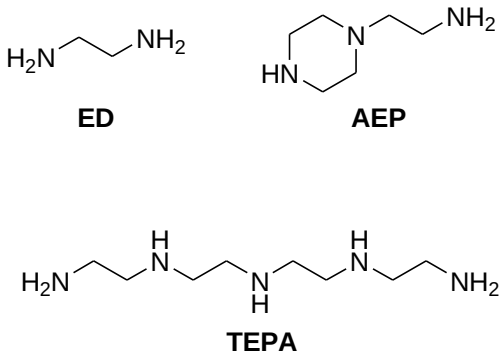

Figure 2. Multi-functional amines used to bind gold cations to the surface of cross-linked polymer SU-8.

Results and Discussion

3.1. Characterization of particles formed by $NaBH_4$ reduction

Figure 3 shows a plan-view bright-field TEM image of Au NPs generated on (and near) the surface of a polymer film by reduction of gold ions bound at the surface using ED then reduced using $NaBH_4$. Element-analysis line scans obtained during plan-view imaging, as well as cross-sectional imaging discussed below, consistently indicate the round high-contrast features are gold. Au NPs form on or near the surface, randomly distributed, with almost no aggregation and no long range order. HAADF-STEM images like that shown in Fig. 4 were analyzed to obtain estimates for the shape and size of particles formed by $NaBH_4$ reduction. Comparison of similar plan-view and cross-sectional images indicate that the dispersion in particle size and spatial homogeneity seen in Fig. 4 is characteristic of the sample.

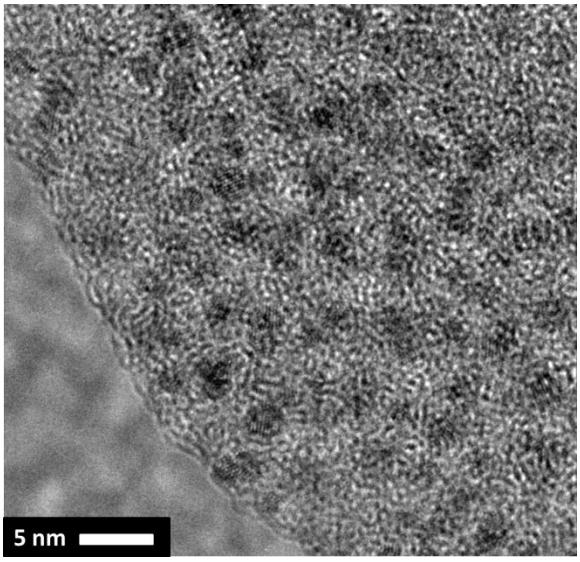

Figure 3. Bright-field plan-view TEM micrograph of Au NPs generated on the polymer by reduction of gold ions bound at the surface by ED then reduced with $NaBH_4$.

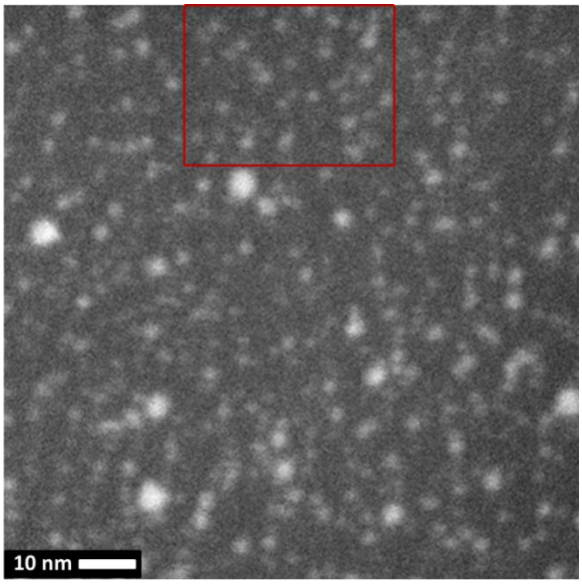

Figure 4. HAADF-STEM image of $NaBH_4$-generated Au NPs. The outlined portion is one of several regions selected for estimating the average number of gold atoms per unit area.

Based on the particle-size analysis, Au NPs formed by $NaBH_4$ reduction are best described as oblate spheroids. Integrate pixel intensity measurements yield an average volume of 8.5 nm^3, with a standard deviation (width of particle volume distribution) of 4.8 nm^3, or an RSD of 60%. This wide distribution arises from large variation observed in both the lateral and vertical radii of the particles. The measured particle heights (normal to the surface) have an average of 1.8 nm with an RSD of 40%, the average lateral radius is 1.4 nm with a RSD of 21%. From these values, one can calculate an average particle volume from height of 7.3 nm^3, in good agreement with the value obtained from integrated pixel intensities.

These particle sizes are comparable to that obtained by synthesis of Au NPs in solution[19,20] and other reports of Au NP generation *in situ* using $NaBH_4$.[28,29,31] Individual particles appear to be spheroids. Although minor faceting can be observed for select particles, as

a whole they appear to be agglomerations of gold atoms, which also lack a definite periodicity. However, by the very nature of the present work, the Au NPs are always viewed against a background of amorphous polymer that significantly reduces contrast relative to that achievable in conventional TEM imaging, where samples are supported on a thin grid. Consequently, the Au NPs may in fact have a definite atomic periodicity that is simply not visible in most nanoparticles. Petkov and co-workers have given evidence that 1.6-nm diameter Au NPs produced by $NaBH_4$ reduction lack periodicity when immersed in solvent, and upon its removal they evolve toward a crystalline structure.[44] It is intriguing to think then that the Au NPs discussed here may in fact be largely amomorphous, consistent with the work of Petkov and *et al*.

3.2. Gold ion coverage and implications for nanoparticle growth

The average number of gold atoms per unit surface-area was estimated from a count of nanoparticles found in representative regions of the HAADF-STEM images. One example of a region used for particle-counting is outlined in red in Fig. 4. The gold atoms were assumed to adopt face-center-cubic packing within the nanoparticles. Using the mean particle volume and the number of particles per region, the gold atom surface density was found to be 10 to 13 atoms nm^{-2} across five different regions, with a mean surface density of 12 atoms nm^{-2}.

Now let us assume that prior to reduction the gold atoms are present as square-planar $AuCl_4^-$ anions hexagonally close-packed on the surface as oblate ellipsoids oriented so the long axis is normal to the surface. Under these assumptions, the gold-ion packing density is approximately 6 atoms nm^{-2}. Thus, the Au NP-decorated polymer surface contains twice as many gold atoms per unit area than could be derived from the densest possible packing of

precursor gold ions on the surface alone. This represents a lower limit, given that the packing arrangement assumed is even denser than that of crystalline $KAuCl_4 \cdot 2H_2O$.[45]

The analysis suggests that either Au ions aggregate on the surface, or more likely, they diffuse into the polymer matrix, so that the polymer functions as a reservoir for gold ions during *in-situ* reduction at the surface. Support for the latter hypothesis can be found from cross-sectional images of the samples, like that in Fig. 5A, which show that most of the Au NPs produced by $NaBH_4$ reduction are not actually *on* the surface, but rather are buried within the polymer matrix at a depth as much as 20 nm below the interface. This in turn implies that both metal ions and the reducing agent can penetrate into the polymer matrix. It is well documented that solvents can swell cross-linked polymers, including SU-8,[46-51] and this effect can be used to chemically modify polymeric surfaces.[52,53] As such, it is perhaps not surprising that both the metal ion source and the reducing agent $NaBH_4$ appear to penetrate into the polymer matrix.

Significantly, these observations suggest that commonly used models which show *in-situ* reduction occurring at the interface of a polymeric surface are overly simplistic and potentially misleading. Other types of surface chemistry conducted at polymeric surfaces may likewise involve diffusion of species into the polymeric matrix, and the matrix itself may be equally or more important to the progress of such reactions as the solution medium at the interface. The study by Khalid *et al.* using a thin polymer layer of trimethoxysilylpropyl-modified polyethylenimine reported similar particle sizes and degrees of surface coverage, which may indicate the interpretation offered here is also applicable to that system.[1]

3.3. Effect of reducing agent on nanoparticle size and position relative to the surface

The observations of Section 3.2 raise the question of how the choice of reducing agent itself affects the formation of NPs at the polymer surface. To explore this further, we examined how the choice of reducing agent affects the size and shape of Au NPs generated and their resulting distribution laterally at (or near) the surface and vertically with respect to the polymer interface. In addition to $NaBH_4$, sodium citrate and hydroquinone were selected for this portion of the study as they are widely used for metal cation reduction and preparing Au NPs in solution.[10,19,20,23,24,31,54]

The TEM cross-sectional images of Fig. 5 show that the size and distribution of Au NPs generated at the surface of the polymer film using $NaBH_4$, sodium citrate, and hydroquinone. It is immediately obvious that the size of Au NPs generated varies substantially, depending upon the reducing agent employed. $NaBH_4$ generates Au NPs in a band that spans from the interface into the polymer film to a depth of approximately 20 nm. As discussed above, these particles are mostly small (radius less than 5 nm), and they appear uniform in size throughout the band. Citrate-generated Au NPs appear to form in two distinct bands of significantly different sizes, and both are larger than those generated with $NaBH_4$. The first band consists of large Au NPs (radius > 5 nm) located at the polymer interface. The second band consists of small Au NPs, comparable in size to those generated by $NaBH_4$, that are spread across a band approximately 40 nm wide and centered about 20 nm below the polymer interface. Reduction with hydroquinone appears to generate only the larger Au NPs having a diameter of 10 nm - 20 nm, consistent with reports of synthesis of Au NPs in solution using hydroquinone.[31] Interestingly,

Au NPs generated with hydroquinone appear to be located in a *single* band located at or very near (within 10 nm) the polymer interface.

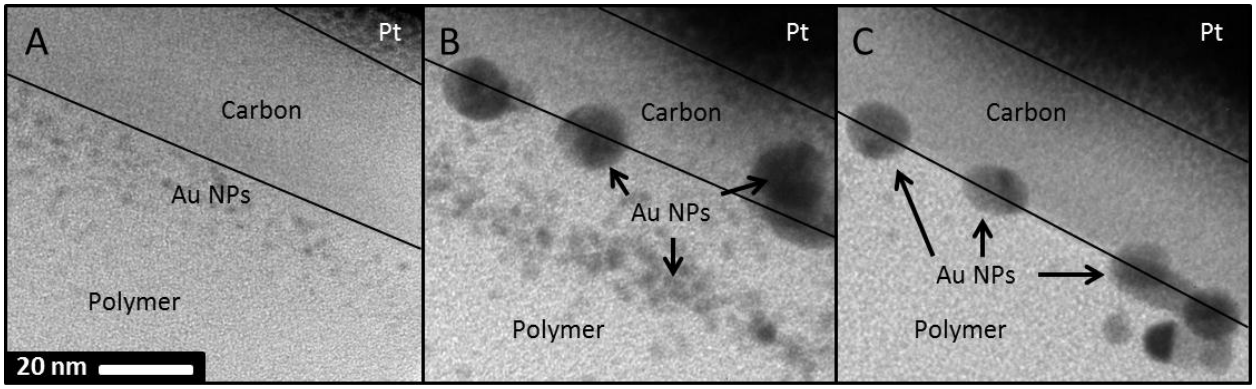

Figure 5. TEM bright-field cross-sectional images of Au NP decorated films prepared using (A) NaBH4, (B) sodium citrate, and (C) hydroquinone. The scale bar is applicable to all images.

The dramatic difference in size of particles generated at versus below the interface may result from the large difference in species mobility within the polymer matrix versus at the interface, as well as variation in strength of the reducing agents. Studies in solution show that strong reducing agents promote formation of small Au NPs because rapid reduction favors nucleation over diffusion limited growth of larger particles.[55-57] The standard reduction potentials of $NaBH_4$ and hydroquinone are -1.37 V and 0.715 V, respectively.[58,59] Consistent with this, the smallest Au NPs observed in this work are generated by $NaBH_4$, the strongest reducing agent used.

The TEM cross-sections show that both $NaBH_4$ and sodium citrate are capable of diffusing into the polymer matrix sufficient to generate Au NPs below the surface. In contrast, hydroquinone generates Au NPs only at or near the polymer interface. Relative to $NaBH_4$ and

sodium citrate, the greater rigidity and steric bulk of hydroquinone may reduce its ability to penetrate the polymer matrix, so that Au NPs are only generated by hydroquinone at the surface.

The outcome of reduction by citrate is intermediate between that observed with $NaBH_4$ and hydroquinone, in that small Au NPs are generated below the polymer surface interface, yet large Au NPs are produced at the interface as well. Au ions located at the surface are expected to have higher mobility. This should favor particle growth over nucleation, especially with weaker reducing agents. Consequently, Au NPs generated at the surface with both sodium citrate and hydroquinone are much larger than those generated within the polymer matrix. Comparing the size of Au NPs produced within the polymer matrix reveals they are larger when produced with citrate than with $NaBH_4$, consistent with the former being the weaker reducing agent. Interestingly, both the large and the small Au NPs observed for *in-situ* reduction by citrate are within the range of sizes observed when prepared in solution (5 - 147 nm), albeit at different reactant concentrations.[8,10,18,19,23] This implies that the polymer matrix does not block Au NP formation, but it does affect particle sizes, which is ascribed to diffusion-limited transport of both gold ions and the reducing agent. This work shows then that the size of Au NPs generated at a polymer surface by *in-situ* reduction and their distribution in depth relative to the interface can be controlled by choice of the reducing agent.

3.4. Influence of binding agent functionalization on nanoparticle depth

Alternative binding agents and surface functionalization chemistry were examined as means for confining gold-ion binding and subsequent Au NP formation to the polymer interface. Ethanol was replaced by water as the solvent for reacting amines with the polymer because water does not swell SU-8,[46-48] so it should reduce transport of the binding agent into the polymer

matrix. Additionally, the alternative binding agents AEP and TEPA were used in place of ED on the assumption that their larger size would decrease their ability to penetrate into the polymer matrix, much as is observed when hydroquinone is the reducing agent. These experiments were performed with $NaBH_4$ as the reducing agent and were otherwise identical in all other ways to procedures described above.

When either aqueous AEP or TEPA is used for binding agent attachment, the Au NPs form in a single layer at the interface approximately one particle-width thick (compare Figs. 6A and 6B with 5A). If the larger amines were able to penetrate into the polymer under aqueous condition and bind gold ions below the surface, or if gold ions could embed within the polymer matrix unbound by the amine, then small Au NPs should have been observed, as in Fig. 5A. The absence of Au NPs substantially below the interface provides supports the hypothesis that TEPA and AEP are unable to penetrate significantly into the polymer matrix and that these larger amines bind gold ions at the interface. Additionally, because the Au NPs that do form at the interface are comparable in size to those observed in Fig. 5A, it provides additional evidence that the size is largely determined by the strength of the reducing agent. This approach decouples the effect of the reducing agent on influencing size of the NPs and the depth at which they form. By using larger binding agents and functionalizing the surface in water, formation of Au NPs can be confined to the surface, whereas their size can be independently selected by parameters of the reduction chemistry that include, but are not limited to, the strength of the reducing agent itself.

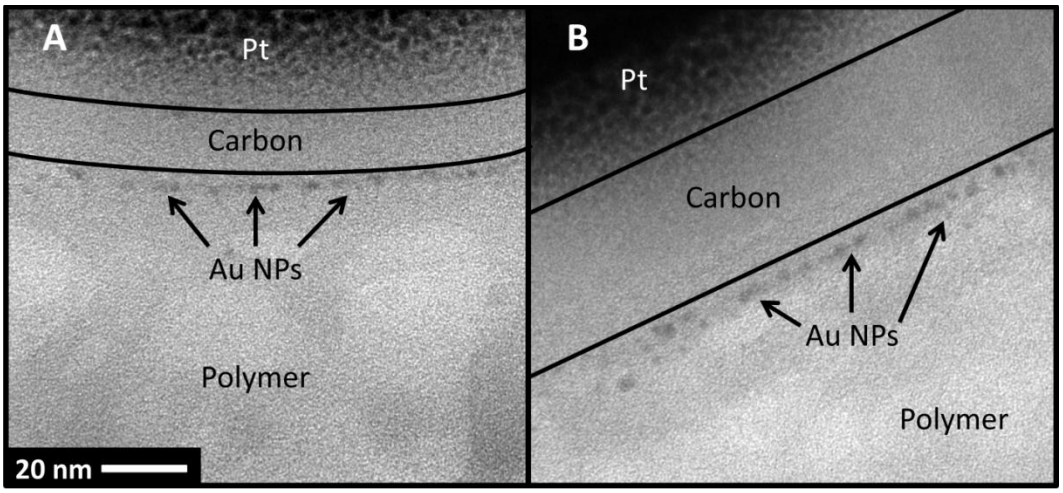

Figure 6. TEM cross-sections of Au NPs created when the polymer is functionalized with the alternative binding (A) AEP and (B) TEPA in water. The scale bar applies to both images. Note that the NP-band is only one particle wide.

3.5. Characterization of surface-bound gold-cation intermediate

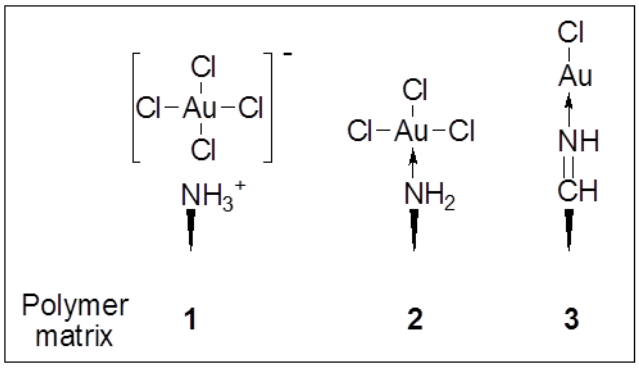

Figure 7. Possible modes for chemisorption of gold cations to the amine-functionalized polymer surface, both at and below the interface.

At least three bonding modes (Fig. 7) can be identified for chemisorption of gold cations to the amine-functionalized polymer. Interestingly, these include neutral and charged Au(I) and Au(III) species. (1) Ion pairing of $AuCl_4^-$ with a protonated amine could form a charged Au(III) species. (2) The amine could displace a chloride ligand forming a covalently bound neutral

Au(III) species. And by analogy with the known reaction of $AuCl_4^-$ with *n*-alkylamines in solution,[60] (3) the amine could partially reduce Au(III) to Au(I) with concomitant loss of HCl and formation of an Au(I)-imine complex. To identify the most likely bonding mode, XPS spectra were obtained for SU-8 films aminated with ED then treated with $HAuCl_4$, as well as non-aminated SU-8 films onto which $HAuCl_4$ was deposited by evaporation of an aqueous solution. These spectra were compared to literature XPS data for reference compounds containing Au(III), Au(I), and Au(0) species.[61]

Analysis of the XPS spectra shows that gold bound to aminated SU-8 exists primarily in the +1 oxidation state (70% to 100% found in four separate samples), whereas the remainder is present in the +3 oxidation state (Fig. 8A). The Au/Cl atom ratio is consistently near unity, after factoring out the one-to-four contribution expected for the fraction of Au(III) observed in a given sample. Following formation of Au NPs (Fig. 8B), gold atoms are detected only as Au(0), and no Cl is found. These observations are consistent with gold ions binding covalently to the aminated polymer predominantly as the Au(I)-imine complex shown in Fig. 7. Secondary and tertiary amines, have been shown capable of reducing $AuCl_4^-$ to Au(0), forming Au NPs, [34,62-64] whereas primary amines cannot.[63,64] This was explained by noting that the oxidation potential of primary amines lies between that of Au(I) and Au(0). This is consistent with our observation that gold bound to an ethylamine-functionalized surface is present in the +1 oxidation state. It also provides an explanation for an observation by Khalid *et al.*, who found significant Au(0) after reacting $AuCl_4^-$ with surfaces bearing a polymer containing secondary amines.[1]

The conclusion that amine-bound gold is present in the +1 oxidation state, perhaps as the gold-imine complex depicted by bonding mode (3), is significant because reports to date assume

gold chemisorbs via bonding mode (1) or (2) only.[31,65-67] It follows then that subsequently reacting such Au(I)-functionalized surfaces with a reducing agent serves only to complete reduction to Au(0), so that the overall formation of surface-bound Au NPs proceeds via a mechanism that differs substantially from that achieved in solution by direct reduction from Au(III). A deeper understanding of this process may enable routes to a range of otherwise inaccessible NP sizes and morphologies.

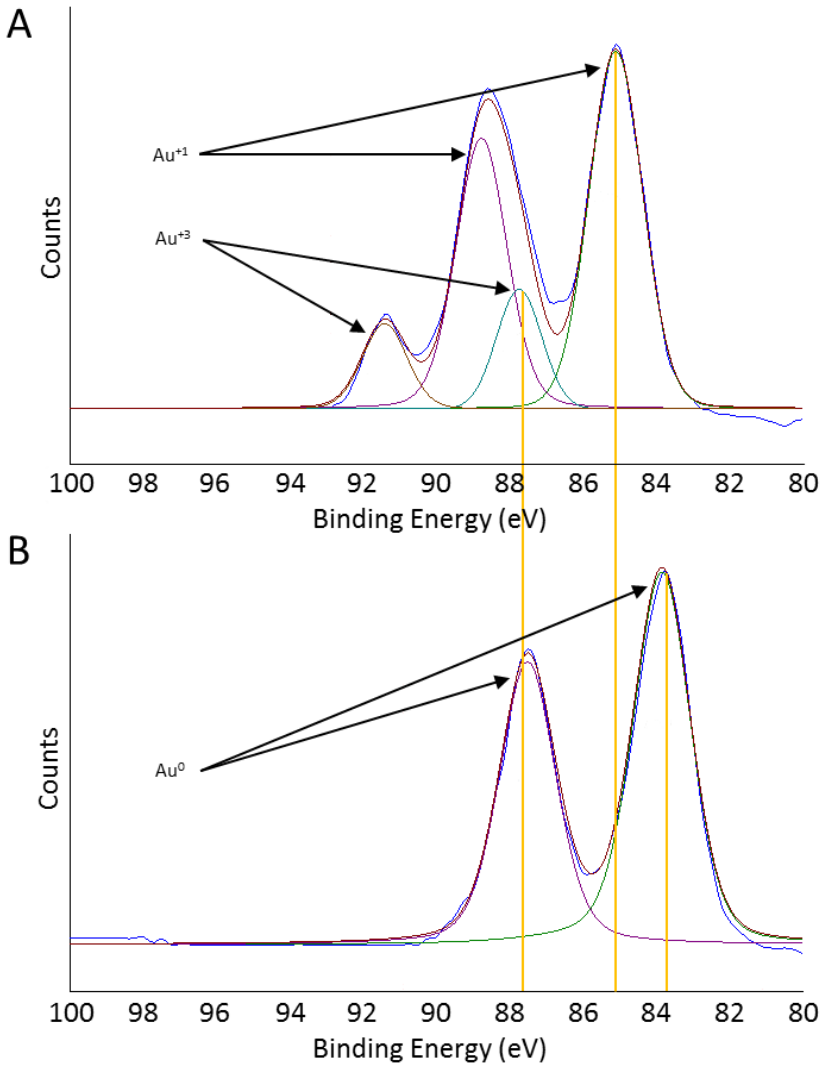

Figure 8. XPS spectra of gold bound to cross-linked SU-8 polymer films. (A) Aminated polymer treated with HAuCl4. (B) Aminated polymer treated with HAuCl4 then reduced with NaBH4 to form Au NPs. The blue line represents the smoothed experimental data. The red line is a curve fit obtained by summing one or more Gaussian-Lorentzian doublets (remaining colors) which correspond to the three possible oxidation states of gold. The gold lines indicate the locations of the primary peaks used to represent the Au oxidation states.

Conclusion

This work shows that synthesizing Au NPs at a cross-linked polymer surface by *in-situ* reduction of metal cations does not necessarily generate particles solely at the liquid-polymer interface. Reducing agents commonly used to synthesize NPs in solution, such as $NaBH_4$ and citrate, can generate particles within cross-linked SU-8 as much as 40 nm below the surface. In contrast, hydroquinone appears to generate NPs only at the interface. It is proposed that diffusion of the metal cation and the reducing agent through the polymer matrix affects the size of Au NPs formed and the depth at which they are generated, and that this can be controlled through the choice of reducing agent and the chemistry used to attach multi-functional amines that bind Au to the polymer. Conditions that encourage attachment of the binding agent to the surface likewise favor Au ion binding and subsequent Au NP generation at the interface, even when $NaBH_4$ is used as the reducing agent. NPs generated at the interface by citrate and hydroquinone are much larger than those generated below the surface, potentially because diffusion of Au ions at the interface is rapid, thereby favoring growth over nucleation. This, too, can be controlled through choice of the reducing agent. When the strong reducing agent $NaBH_4$ is reacted with Au ions bound at the interface, the rapid reaction favors nucleation over growth yielding small NPs. Particles generated by *in-situ* reduction with $NaBH_4$ on SU-8 are shown to be oblate spheroids.

These results have immediate significance because the model polymer SU-8 is a high-performance cross-linkable epoxide polymer that is increasingly employed for micro- and nano-scale fabrication of high-aspect ratio structures and functional devices. Additionally, the results suggest it may be possible to control synthesis of Au NPs below the interface of a polymer. This

could be useful for several emerging applications in photonics. For example, it is well know that metal NPs can be used to achieve dramatic field enhancement of optical effects.[68-70] In the case of fluorescence, the overall emission enhancement is optimized at a certain distance from the NP, because absorption enhancement and NP-induced quenching are competing effects that exhibit different distance dependence.[71] As such, controlling the depth at which Au NPs are created below a surface by the method reported here may be useful for creating material systems with controlled optical enhancement that are not compromised by fluorescence quenching.

The findings in this work indicate that *in situ* NP synthesis -- and perhaps many other types of chemistry performed at a polymer surface -- are not true surface chemistry, as the process is not restricted to the polymer interface. As such, it provides insight that should further development of more accurate models and improve application of processes for functionalizing polymeric interfaces. To that end, note that the polymer matrix appears to function as a reservoir for metal ions for *in-situ* reduction, consequently the kinetics of NP generation should depend upon diffusion of metal ions within the matrix and to the surface, as well as diffusion of certain reducing agents into the matrix. Because Au NPs can be seen *within* the polymer matrix, it suggests that many of the particles are actually generated within the polymer, and not truly on the surface in a solution matrix. It follows then that the role of the polymer matrix may be important in determining, or even controlling, the shape, size, and properties of the NPs generated. The effects discussed here may be even more significant for non-cross-linked materials, such as poly(methylmethacrylate) (PMMA), which are also commonly employed for creating surface-functionalized micro- and nano-scale devices. These are all areas for further fruitful study.

References

(1) Khalid, M.; Pala, I.; Wasio, N.; Bandyopadhyay, K. *Colloid. Surface. A* **2009**, *348*, 263.

(2) Zhang, Q.; Xu, J.-J.; Liu, Y.; Chen, H.-Y. *Lab Chip* **2008**, *8*, 352.

(3) Zhao, W.; Sun, S.-X.; Xu, J.-J.; Chen, H.-Y.; Cao, X.-J.; Guan, X.-H. *Anal. Chem.* **2008**, *80*, 3769.

(4) He, H.; Cai, W.; Lin, Y.; Chen, B. *Langmuir* **2010**, *26*, 8925.

(5) Kisailus, D.; Najarian, M.; Weaver, J. C.; Morse, D. E. *Adv. Mater.* **2005**, *17*, 1234.

(6) Rahman, M. A.; Son, J. I.; Won, M.-S.; Shim, Y.-B. *Anal. Chem.* **2009**, *81*, 6604.

(7) Henry, A. C.; McCarley, R. L. *J. Phys. Chem. B* **2001**, *105*, 8755.

(8) Li, W.-C.; Park, S.-E.; Kim, J.; Lee, S.-W. *Jpn. J. Appl. Phys.* **2009**, *48*, 06FF14.

(9) Tian, B.; Xie, P.; Kempa, T. J.; Bell, D. C.; Lieber, C. M. *Nat. Nanotechnol.* **2009**, *4*, 824.

(10) Grabar, K. C.; Freeman, R. G.; Hommer, M. B.; Natan, M. J. *Anal. Chem.* **1995**, *67*, 735.

(11) Sreeprasad, T. S.; Pradeep, T. *Langmuir* **2011**, *27*, 3381.

(12) Cooper, G. M. *The Cell: A Molecular Approach*; ASM Press: Washington DC, 1997.

(13) Guo, B.; Zhao, S.; Han, G.; Zhang, L. *Electrochim. Acta* **2008**, *53*, 5174.

(14) Kreitz, S.; Penache, C.; Thomas, M.; Klages, C. P. *Surf. Coat. Tech.* **2005**, *200*,

676.

(15) Qiu, J.; Guo, M.; Feng, Y.; Wang, X. *Electrochim. Acta* **2011**, *56*, 5776.

(16) Ng, J. H. G.; Desmulliez, M. P. Y.; Prior, K. A.; Hand, D. P. *Micro Nano Lett.* **2008**, *3*, 82.

(17) Huo, S.-J.; Xue, X.-K.; Li, Q.-X.; Xu, S.-F.; Cai, W.-B. *J. Phys. Chem. B* **2006**, *110*, 25721.

(18) Ojea-Jimenez, I.; Romero, F. M.; Bastús, N. G.; Puntes, V. *J. Phys. Chem. C* **2010**, *114*, 1800.

(19) Daniel, M.-C.; Astruc, D. *Chem. Rev.* **2004**, *104*, 293.

(20) DiScipio, R. G. *Anal. Biochem.* **1996**, *236*, 168.

(21) Kobayashi, Y.; Tadaki, Y.; Nagao, D.; Konno, M. *J. Colloid Interf Sci.* **2005**, *283*, 601.

(22) Liu, B.; Li, Q.; Zhang, B.; Cui, Y.; Chen, H.; Chen, G.; Tang, D. *Nanoscale* **2011**, *3*, 2220.

(23) Turkevich, J.; Stevenson, P. C.; Hillier, J. *J. Phys. Chem.* **1953**, *57*, 670.

(24) Gómez-Lahoz, C.; García-Herruzo, F.; Rodríguez-Maroto, J. M.; Rodríguez, J. J. *Separ. Sci. Technol.* **1992**, *27*, 1449.

(25) Ishida, T.; Kuroda, K.; Kinoshita, N.; Minagawa, W.; Haruta, M. *J. Colloid Interf. Sci.* **2008**, *323*, 105.

(26) Tal, A.; Chen, Y.-S.; Williams, H. E.; Rumpf, R. C.; Kuebler, S. M. *Opt. Express* **2007**, *15*, 18283.

(27) Chen, X.; Zhao, D.; Zhao, L.; An, Y.; Ma, R.; Shi, L.; He, Q.; Chen, L. *Sci. China*

Ser. B **2009**, *52*, 1372.

(28) Li, S.-N.; Yang, X.-L.; Huang, W.-Q. *Chinese J. Polym. Sci.* **2007**, *25*, 555.

(29) Liu, Y.; Cheng, S. Z. D.; Wen, X.; Hu, J. *Langmuir* **2002**, *18*, 10500.

(30) Peng, Z.; Wang, E.; Dong, S. *Electrochem. Commun.* **2002**, *4*, 210.

(31) Zhong, L.; Jiao, T.; Liu, M. *Langmuir* **2008**, *24*, 11677.

(32) Xu, Y.; Cao, Q.; Svec, F.; Fréchet, J. M. J. *Anal. Chem.* **2010**, *82*, 3352.

(33) Pong, F. Y.; Lee, M.; Bell, J. R.; Flynn, N. T. *Langmuir* **2006**, *22*, 3851.

(34) Newman, J.; Blanchard, G. *J. Nanopart. Res.* **2007**, *9*, 861.

(35) Mata, A.; Kim, E. J.; Boehm, C. A.; Fleischman, A. J.; Muschler, G. F.; Roy, S. *Biomaterials* **2009**, *30*, 4610.

(36) Yeo, J.-S.; Lewis, H.; Meyer, N. *J. Laser Micro/Nanoeng.* **2007**, *2*, 31.

(37) Yang, R.; Lu, B.-R.; Xue, J.; Shen, Z.-K.; Xu, Z.-C.; Huq, E.; Qu, X.-P.; Chen, Y.; Liu, R. *Microelectron. Eng.* **2010**, *87*, 824.

(38) Chen, Y.-S.; Tal, A.; Kuebler, S. M. *Chem. Mater.* **2007**, *19*, 3858.

(39) Farrer, R. A.; LaFratta, C. N.; Li, L.; Praino, J.; Naughton, M. J.; Saleh, B. E. A.; Teich, M. C.; Fourkas, J. T. *J. Am. Chem. Soc.* **2006**, *128*, 1796.

(40) Danscher, G. *Histochemistry* **1981**, *71*, 81.

(41) Briggs, D. *Surface Analysis of Polymers by XPS and Static SIMS*; Cambridge University Press: Cambridge, U.K. ; New York, 1998.

(42) Bêche, B.; Papet, P.; Debarnot, D.; Gaviot, E.; Zyss, J.; Poncin-Epaillard, F. *Opt. Commun.* **2005**, *246*, 25.

(43) Wagner, C. D.; Muilenberg, G. E. *Handbook of X-Ray Photoelectron*

Spectroscopy: a Reference Book of Standard Data for Use in X-Ray Photoelectron Spectroscopy; Perkin-Elmer Corp., Physical Electronics Division, 1979.

(44) Petkov, V.; Bedford, N.; Knecht, M. R.; Weir, M. G.; Crooks, R. M.; Tang, W.; Henkelman, G.; Frenkel, A. *J. Phys. Chem. C.* **2008**, *112*, 8907.

(45) Theobald, F.; Omrani, H. *Acta Crystallogr. B* **1980**, *36*, 2932.

(46) Wouters, K.; Puers, R. *J. Micromech. Microeng.* **2010**, *20*, 095013.

(47) Liu, C.; Liu, Y.; Sokuler, M.; Fell, D.; Keller, S.; Boisen, A.; Butt, H.-J.; Auernhammer, G. K.; Bonaccurso, E. *Phys. Chem. Chem. Phys.* **2010**, *12*, 10577.

(48) Wouters, K.; Puers, R. *Procedia Chem.* **2009**, *1*, 60.

(49) Wang, Y.; Monch, W.; Aatz, B.; Zappe, H. *J. Micromech. Microeng.* **2010**, *20*, 15003.

(50) Hill, G. C.; Melamud, R.; Declercq, F. E.; Davenport, A. A.; Chan, I. H.; Hartwell, P. G.; Pruitt, B. L. *Sensor. Actuat. A-Phys.* **2007**, *138*, 52.

(51) Hsieh, J.; Weng, C. J.; Yin, H. L.; Lin, H. H.; Chou, H. Y. *Microsyst. Technol.* **2005**, *11*, 429.

(52) Kim, H.-N.; Kang, J.-H.; Jin, W.-M.; Moon, J. H. *Soft Matter* **2011**, *7*, 2989.

(53) Ford, J.; Marder, S. R.; Yang, S. *Chem. Mater.* **2009**, *21*, 476.

(54) Sirajuddin; Mechler, A.; Torriero, A. A. J.; Nafady, A.; Lee, C.-Y.; Bond, A. M.; O'Mullane, A. P.; Bhargava, S. K. *Colloid. Surface. A* **2010**, *370*, 35.

(55) Shankar, R.; Shahi, V.; Sahoo, U. *Chem. Mater.* **2010**, *22*, 1367.

(56) Troupis, A.; Triantis, T.; Hiskia, A.; Papaconstantinou, E. *Eur. J. Inorg. Chem.* **2008**, *2008*, 5579.

(57) Reetz, M. T.; Maase, M. *Adv. Mater.* **1999**, *11*, 773.

(58) Song, Y.; Xie, J.; Song, Y.; Shu, H.; Zhao, G.; Lv, X.; Xie, W. *Spectrochim. Acta A* **2006**, *65*, 333.

(59) Celon, E.; Bresadola, S. *Microchim. Acta* **1969**, *57*, 441.

(60) Nagel, Y.; Beck, W. *Z. Anorg. Allg. Chem.* **1985**, *529*, 57.

(61) Fong, Y.-Y.; Visser, B. R.; Gascooke, J. R.; Cowie, B. C. C.; Thomsen, L.; Metha, G. F.; Buntine, M. A.; Harris, H. H. *Langmuir* **2011**, *27*, 8099.

(62) Aslam, M.; Fu, L.; Su, M.; Vijayamohanan, K.; Dravid, V. P. *J. Mater. Chem.* **2004**, *14*, 1795.

(63) Newman, J. D. S.; Blanchard, G. J. *Langmuir* **2006**, *22*, 5882.

(64) Richardson, M. J.; Johnston, J. H.; Borrmann, T. *Eur. J. Inorg. Chem.* **2006**, *2006*, 2618.

(65) Pandikumar, A.; Murugesan, S.; Ramaraj, R. *ACS App. Mater. Inf.* **2010**, *2*, 1912.

(66) Kim, Y.-G.; Oh, S.-K.; Crooks, R. M. *Chem. Mater.* **2003**, *16*, 167.

(67) Chia, K.-K.; Cohen, R. E.; Rubner, M. F. *Chem. Mater.* **2008**, *20*, 6756.

(68) Jain, P. K.; Huang, X.; El-Sayed, I. H.; El-Sayed, M. A. *Plasmonics* **2007**, *2*, 107.

(69) Zou, S.; Schatz, G. C. *Isr. J. Chem.* **2006**, *46*, 293.

(70) Mishra, H.; Zhang, Y.; Geddes, C. D. *Dyes Pigments* **2011**, *91*, 225.

(71) Eustis, S.; El-Sayed, M. A. *Chem. Soc. Rev.* **2006**, *35*, 209.